Evaluating the Ultimate Performance of Pylon-Head Joints with Numerical Analysis

Wael A. Salah
Department of Civil Engineering, Engineering College, Northern Border University, Arar, Saudi Arabia | Department of Civil Engineering, Faculty of Engineering, Al-Azhar University, Cairo, Egypt
wael.khalil@nbu.edu.sa (corresponding author)

Moustafa S. Darweesh
Department of Civil Engineering, Engineering College, Northern Border University, Arar, Saudi Arabia
mustafa.samir@nbu.edu.sa

Received: 26 April 2024 | Revised: 8 May 2024 | Accepted: 20 May 2024

 DOI: https://doi.org/10.48084/etasr.7652

ABSTRACT

This study presents a comprehensive Finite Element (FE) model of the multiple-cable-to-pylon head joint within a specific cable roof structure. The analysis focuses on the upper part of the pylon substructure, particularly the pylon head joint, to examine its localized behavior under a set of internal forces derived from a simplified FE model. The steel tubular components of the pylon substructure were precisely simulated using thin shell elements. The designers of this particular roof structure proposed two solutions for reinforcing the pylon-head joint, while an additional novel strengthening technique was introduced, aimed at enhancing the joint's performance. These three strengthening methods, along with the original design joint, were modeled numerically, and the joint's effectiveness was assessed. The findings of the analysis indicate that the newly proposed strengthening technique exhibits greater potential for stiffening the considered pylon-head joint compared to the other introduced solutions. The study concludes with significant insights relevant to practical applications.

Keywords- pylon-head joint; finite element analysis; failure load; cable roof structure; joint strength

I. INTRODUCTION

Steel cables and membrane structures offer an optimal solution for covering large spans without internal supports. This specific structural system transfers all developed internal forces through pre-tensioned cable components, along with the compression ring and pylon support system. These systems have proven to be just as effective as the textile surface membrane structures and reinforced concrete shell structures. To ensure structural safety and integrity, the surface membrane and cable elements must meet specific criteria for weight, balance, strength, stiffness, and durability. These characteristics enable the stress distribution to align with external loading conditions in an elastic stage, preventing excessive localized plastic deformations in the steel supporting elements. Addressing the challenges of force transmission in cable roof structures requires meticulous attention to localized stress concentrations and the stiffness behavior of cable support elements. As this unconventional shell roof with cable structure is not widely adopted, most research has focused on investigating pylon structures within bridge systems, particularly in cable-stayed and suspension bridges. An FE analysis was conducted to evaluate the performance of pylon structures in a cable-stayed bridge [1]. The two pylon structures of the bridge exhibited permanent plastic deformations when subjected to the predetermined design loads. Recommendations were made to reinforce the existing pylon structures, such as increasing the material thickness in critical areas or enhancing material properties by utilizing higher strength materials. Further research focused on investigating the fatigue impact on the cable-to-steel pylon connection [2]. A full-scale specimen of the cable-to-steel pylon connection from a cable-stayed bridge was constructed, and numerous fatigue tests were conducted. No cracks were recorded on the anchor box surface after subjecting it to a 2.76 million fatigue cycle test.

This study introduces an elaborate FE model of the multiple-cable-to-pylon head joint in an actual project. The roof layout, with a focus on the supporting elements, is illustrated in Figure 1. These elements consist of a ring system supported by columns from one side of the roof and two pylons on the other, which secure the ring with cables. Each pylon is composed of three tubular elements that intersect at the top and bottom of the pylon, ascertaining that the pylon acts as a single leaning column. Figure 2 depicts the complex details of the pylon-head joint where the cables are anchored. After assembling the entire structure, the roof underwent testing followed by a final inspection for operational readiness. During this inspection, cracks were discovered in the walls of the spire tubular member near the welded connections to the head member.

Fig. 1. The considered amphitheater's roof with pylons, Poland.

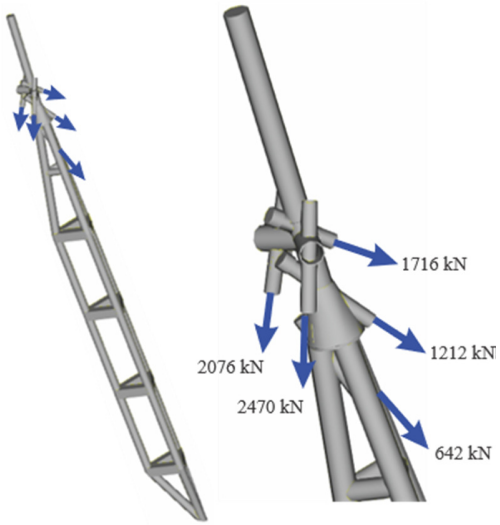

Fig. 2. The design cable forces of the considered pylon.

The overall structure was simulated as a 3D system consisting of flexible cable elements for transmitting tensile forces and beam elements representing the ring and pylon components. In the design phase, the pylon joints were not thoroughly examined and were dimensioned without a comprehensive analysis of the potential localized yielding of joint components under service applied loads. The intersection of multiple elements in a limited space within the head joint presented difficulties in meeting the required fitting tolerances and certifying the quality of welded connections during manufacturing. Due to limitations of the initial design analysis, which modeled pylon subcomponents as interconnected beam elements and could not fully capture the intricate behavior of such structures, a more advanced FE modeling approach becomes essential to assess the ultimate strength of such complex structural systems. FE analysis was carried out to assess the performance of the initial design iteration of the head joint, as evidenced in Figure 2, along with two strengthened versions suggested by the designer (joints strengthened with supplementary hollow conical elements to support the spire tube).

A particular set of internal forces generated in the upper portion of the pylon, based on the entire roof model, was selected for an in-depth analysis of the localized behavior of the pylon-head joint. This joint incorporates the guiding elements of a Circular Hollow Section (CHS) for the roof cables anchored within the pylon. Moreover, the pylon's upper CHS spire element facilitates the secure transfer of loads from the roof cables to the compound pylon composed of three chord and batten tubular members. Figure 3 provides a representation of the pylon and its subsystem, with a focus on the head joint under investigation in this study to identify failure modes, strength characteristics, and plastic zones in the ultimate state.

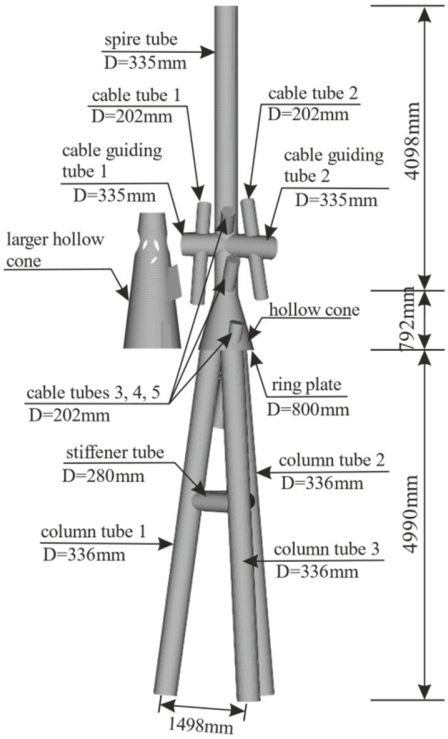

Fig. 3. Component of pylon-head joint.

II. FE MODELLING

This section presents a detailed FE modeling to predict the strength of the pylon-head joint within the pylon's cable roof. ABAQUS FE software [3] was employed to numerically simulate the performance of the considered pylon-head joint. The FE modeling of the pylon-head joint in ABAQUS deployed a combination of a four-node quadrilateral first order element with full integration and six degrees of freedom in each node (S4) as well as a three-node triangular first order element with full integration and six degrees of freedom in each node (S3) shell elements to model the interconnected steel tubes with complex geometry. S4 elements, effective for thin to moderately thick structures, represented the main geometry, while S3 elements facilitated smooth transitions in regions with uneven distributions of S4 elements, enhancing modeling accuracy. For models requiring high result accuracy, the S4 element offers superior performance compared to some other shell elements [4]. These two shell elements have been widely used in previous studies, demonstrating exceptional ability in capturing the behavior of modeled structures [5-7].

The accuracy of the FE model results is highly dependent on the refinement level of the elements mesh. While refinement improves solution convergence, it incurs a significant computational cost. Therefore, the mesh is refined in critical regions where high stress gradients or solution discontinuities are anticipated, resulting in a more accurate representation of the physical phenomena [8]. A mesh size that balances accuracy and computational cost was utilized, with a uniform element size of 30 × 30 mm for quad elements and a 30 mm edge size for triangular elements. This mesh strategy optimized computational efficiency while ensuring detailed structural analysis under applied loads. The material behavior was described by an elastic-perfectly plastic model, with steel properties including a Young's modulus of 200 GPa, 0.3 Poisson's ratio, and yield stresses of 335 MPa for column and spire tubes and 345 MPa for cable tubes, guiding tubes, stiffener plates, and shell cones.

The analysis focused on four different joint solutions. The first solution involved the initial design, which includes a short, hollow steel cone. The second solution, termed stiffening 1, enhances the original design by reinforcing the short hollow cone with a longer hollow cone of 16 mm thickness welded to the spire tube, cable guiding tubes, and the joint bottom plate. The third solution, known as stiffening 2, introduces an additional reinforcing cover shell of 20 mm thickness welded to the top half of the longer hollow cone. A fourth solution is proposed, with a longer hollow cone and a 16 mm thick stiffener plate connecting cable tube 1 to the external surface of the larger hollow cone. Additionally, the top part of cable tube 2 was reinforced with a 16 mm thick confining tube welded to its top end and its intersection with cable guiding tube 2. These four solutions were numerically modeled, focusing solely on the pylon-head joint. A single loading step containing the design cable forces was applied. The two stiffening solutions proposed by the designer (stiffening 1 and stiffening 2) are depicted in detail in Figures 4 and 5, respectively.

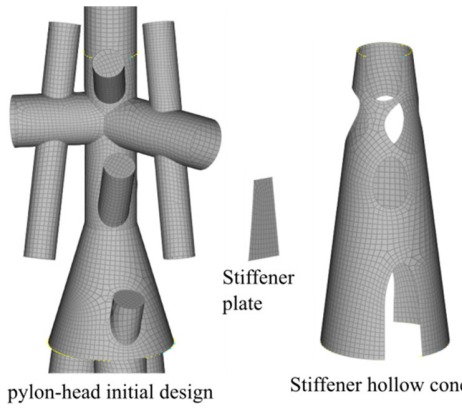

Fig. 4. First considered strengthening technique of the pylon-head joint.

Figure 6 outlines the authors' joint reinforcing proposal. All welded elements in the pylon-head joint were modeled numerically using merged nodes along the circumference of the intersection [9]. For a more thorough examination of the welded components, the welding material could be accurately simulated by employing solid elements to connect the two welded parts. The steel material has 210 GPa Young modulus and 0.3 Poisson ratio. The yield stress of the steel is 345 MPa for the column and the spire tubes and 355 MPa for all the other sub-connection elements. The material behavior was represented as elastic-perfect plastic. Concentrated loads were applied along the axial directions of the cable tubes, as observed in Figure 2. The numerical analysis incorporated both geometric and material nonlinearities. The loading procedures were implemented deploying the Riks analysis featured in ABAQUS to capture the nonlinear characteristics of the analyzed joint. The shell elements used, the aspect ratio implemented, and the material modeling underwent validation in previous research [10-11].

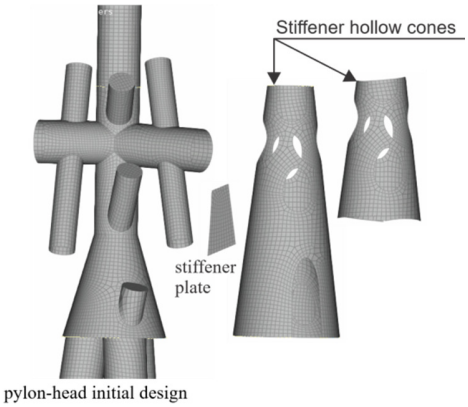

Fig. 5. Second considered strengthening technique of the pylon-head joint.

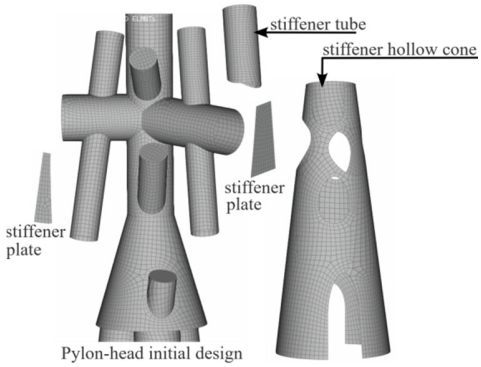

Fig. 6. The proposed stiffening technique.

To assess the sensitivity of the analyzed subsystems to buckling effects and characterize potential initial imperfections, a linear perturbation buckling analysis was executed. The first buckling mode was selected to picture the imperfect geometry of the pylon in its unloaded state [10]. Furthermore, numerical analysis evaluated load-displacement characteristics through Riks analysis, considering both geometric and material nonlinearities. This analysis was performed for two model techniques: a perfect model and an imperfect model that incorporates these nonlinearities alongside initial imperfections. The imperfection option available in ABAQUS was deployed to create the imperfect structure based on the

shape of the first buckling mode obtained from the perturbation analysis.

III. RESULTS OF FE MODELLING

A linear perturbation numerical analysis was initially conducted to identify the potential buckling modes of the pylon-head joint structure. These modes represent the weakest configurations susceptible to buckling under increasing load, expressed as load factors relative to the applied design forces. Figure 7 presents the first buckling mode, which exhibits a critical load factor of a 4.99. Additional buckling modes were found to be close in nature to the first one, with the second and third modes characterized by bifurcation load factors of 5.32 and 5.85, respectively. The analysis was then repeated for the strengthened joint design designated as "stiffened 1". This case displayed a reduced contribution of spire deformation to the overall buckling behavior, with a greater emphasis on localized effects. The first buckling mode for this design achieved a load factor of 5.23, exceeding that of the initial solution. Higher order buckling modes in the strengthened joint maintained similar forms but were primarily associated with localized buckling rather than global pylon deformation. These higher modes exhibited bifurcation load factors of 6.00 and 6.62. Similar behavior was observed for the "stiffened 2" joint configuration. Figure 8 portrays the von Mises stress distribution and the resulting deformations at the failure load for all considered FE models. The final results are showcased in a load-displacement characteristic format, where the load factor of the applied design forces is plotted against the corresponding lateral displacement of the pylon's top end.

Only the results for the pylon-head joint with imperfect geometry are presented here. The nonlinear numerical analysis of the initial design pylon-head joint revealed localized buckling in the spire tube, particularly at the joint with the initial hollow cone, as shown in Figure 8(a). Continued compression caused stable growth of wrinkles, gradually reducing the spire tube's axial rigidity [12]. Initial site inspections observed cracks and wrinkles within the spire tube just above the initial attached cone. This is because the section welded to the base cone represents the critical section of the spire tube. The ultimate strength of the pylon-head joint was reached at only 60% of the design forces, as depicted in Figure 9. The first proposed solution, stiffening 1, reinforced the critical zone of the spire tube by adding a larger hollow cone that confined the base cone and extended to join the spire tube after covering the entire area connected to the subconnection elements. This solution significantly improved the ultimate strength of the joint. Plastification developed and spread along the added larger hollow cone (Figure 8(b)), with 110% of the design forces reached before the joint reached its ultimate strength. The second stiffening solution, stiffening 2, involved adding another hollow cone to confine the top half of the previously added larger hollow cone. This solution did not significantly improve the joint's ultimate strength because the plastification zone shifted to cable tube 2 (Figure 8(c)) at the same load level as in stiffening 1. At a certain stage, the compressed region of the bent cable tube 2 developed axial wrinkles, leading to localized instability [13], explaining the relatively short distance transferred by the top end of the spire tube.

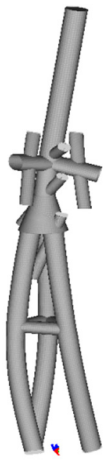

Fig. 7. First buckling mode shape of the original pylon-head joint.

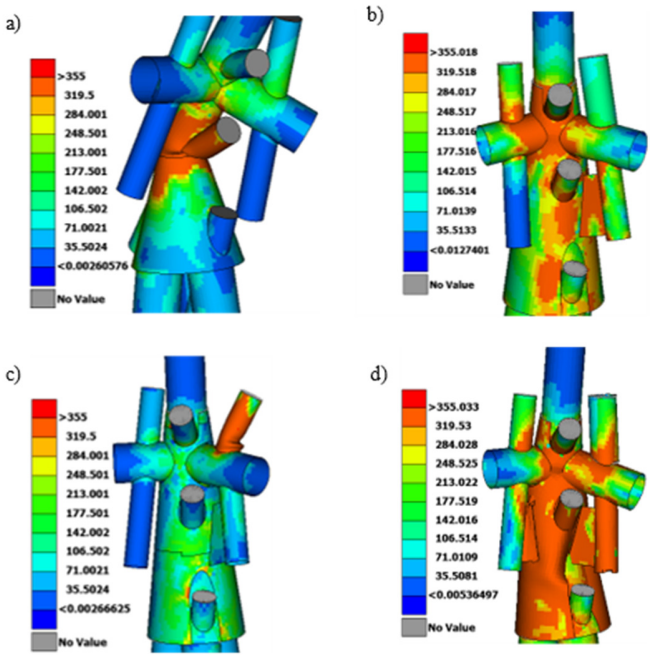

Fig. 8. Von Mises stresses distribution on deformed geometry for the four pylon-head joints considered: (a) original design joint, (b) first stiffened joint, (c) second stiffened joint, (d) proposed joint stiffening.

The proposed solution retained the large hollow cone employed in both stiffening 1 and 2. Additionally, a stiffener plate was introduced to strengthen the joint by connecting cable tube 1 to the large hollow cone. Cable tube 2 was further supported by a 16 mm thick outer jacket tube. This supporting tube was welded to the top end of cable tube 2 on one side and around its intersection with cable guiding tube 2 on the other side. However, cable tube 2 can be reinforced with steel elements of varying cross-sections, as outlined in [14]. The FE analysis results for the proposed solution disclose a significant improvement in the ultimate load strength, reaching 117% of

the design forces, as depicted in Figure 9. Figure 8(d) demonstrates that plastic deformation occurred throughout the larger hollow cone and the cable tubes at ultimate strength, indicating that the proposed solution achieved higher section efficiency.

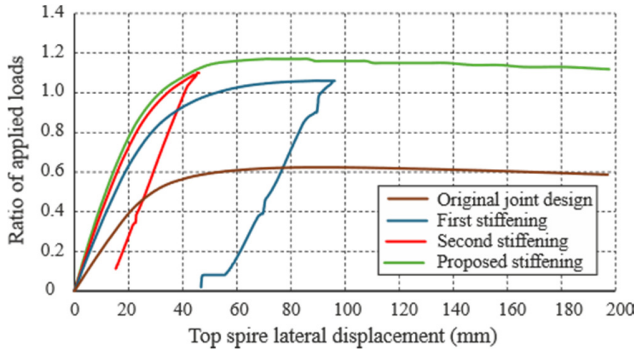

Fig. 9. Top spire lateral displacement against the ratio of applied loads.

IV. CONCLUSIONS

This study presents an advanced analysis of the complex head joint for pylons supporting a cable roof. The original joint design lacked detailed Finite Element (FE) analysis, which could have replicated its behavior under both ultimate and serviceability limit states. This has resulted in the joint being overstressed and failing below the design load level. The insufficient strength of the pylon-head joint prompted significant proposals for joint detailing to meet the limit state criteria for both the ultimate and serviceability limit states. Reinforcements were introduced to the original design in the form of conical shells. This study proposes a new strengthening solution with a longer conical shell, a stiffener plate connecting cable tube 1 to the shell, and a stiffening jacket tube for cable tube 2. The reinforced joints exhibit an ultimate load factor exceeding unity relative to the design forces, ensuring reliability at the ultimate limit state. The proposed solution is considered optimal compared to others due to its enhanced joint efficiency, with all subcomponents reaching yield stress at failure load.

However, to prevent failure under alternating loading, the head joint must undergo minimal plastic deformations, ideally remaining entirely elastic in the serviceability limit state. This crucial requirement is not extensively discussed in the paper. Additionally, conventional FE modeling is deemed inadequate for such a complex structure. More advanced techniques are necessary to accurately capture joint performance, especially with multiple interconnected elements in a confined area.

ACKNOWLEDGMENTS

The authors extend their appreciation to the Deanship of Scientific Research at Northern Border University, Arar, KSA for funding this research work through the project number "NBU-FFR-2024-1946-01").

REFERENCES

[1] M. Akbar and A. S. Nugraha, "Structural Analysis of Pylon Head for Cable Stayed Bridge Using Non-Linear Finite Element Method," *Journal of Ocean, Mechanical and Aerospace -science and engineering-*, vol. 51, no. 1, pp. 1–6, Oct. 2018.

[2] H. Wang, C. Xie, Z. Fan, and S. Qin, "Experimental Study on Fatigue Performance of Cable-to-Steel Pylon Connection," *Iranian Journal of Science and Technology, Transactions of Civil Engineering*, vol. 47, no. 3, pp. 1909–1917, Jun. 2023, https://doi.org/10.1007/s40996-022-00998-4.

[3] T. Belytschko and T. Black, "Elastic crack growth in finite elements with minimal remeshing," *International Journal for Numerical Methods in Engineering*, vol. 45, no. 5, pp. 601–620, 1999, https://doi.org/10.1002/(SICI)1097-0207(19990620)45:5<601::AID-NME598>3.0.CO;2-S.

[4] N. Perera and M. Mahendran, "Finite element analysis and design for section moment capacities of hollow flange steel plate girders," *Thin-Walled Structures*, vol. 135, pp. 356–375, Feb. 2019, https://doi.org/10.1016/j.tws.2018.10.014.

[5] Y. I. Park, J.-S. Cho, and J.-H. Kim, "Numerical and Experimental Investigation of Quasi-Static Crushing Behaviors of Steel Tubular Structures," *Materials*, vol. 15, no. 6, Jan. 2022, Art. no. 2107, https://doi.org/10.3390/ma15062107.

[6] D. Galhofo, N. Silvestre, A. M. de Deus, L. Reis, A. P. C. Duarte, and R. Carvalho, "Structural behaviour of pre-tensioned solar sails," *Thin-Walled Structures*, vol. 181, Dec. 2022, Art. no. 110007, https://doi.org/10.1016/j.tws.2022.110007.

[7] J. Dong and R. Sause, "Flexural strength of tubular flange girders," *Journal of Constructional Steel Research*, vol. 65, no. 3, pp. 622–630, Mar. 2009, https://doi.org/10.1016/j.jcsr.2008.02.019.

[8] P. Natário, N. Silvestre, and D. Camotim, "Web crippling failure using quasi-static FE models," *Thin-Walled Structures*, vol. 84, pp. 34–49, Nov. 2014, https://doi.org/10.1016/j.tws.2014.05.003.

[9] H. A. Le, "A Numerical Study addressing the Stress Distribution in Circular Steel Tube Confined Concrete Columns considering Various Concrete Strengths," *Engineering, Technology & Applied Science Research*, vol. 13, no. 2, pp. 10347–10351, Apr. 2023, https://doi.org/10.48084/etasr.5581.

[10] W. A. Salah, "Performance of Hybrid Castellated Beams: Prediction Using Finite Element Modeling," *Engineering, Technology & Applied Science Research*, vol. 12, no. 2, pp. 8444–8451, Apr. 2022, https://doi.org/10.48084/etasr.4824.

[11] W. A. Salah, "Lateral Torsional Buckling Capacity Assessment of Cellular Steel Beams," *Practice Periodical on Structural Design and Construction*, vol. 28, no. 1, Feb. 2023, Art. no. 04022065, https://doi.org/10.1061/PPSCFX.SCENG-1210.

[12] J. A. Paquette and S. Kyriakides, "Plastic buckling of tubes under axial compression and internal pressure," *International Journal of Mechanical Sciences*, vol. 48, no. 8, pp. 855–867, Aug. 2006, https://doi.org/10.1016/j.ijmecsci.2006.03.003.

[13] F. Guarracino, "On the analysis of cylindrical tubes under flexure: theoretical formulations, experimental data and finite element analyses," *Thin-Walled Structures*, vol. 41, no. 2, pp. 127–147, Feb. 2003, https://doi.org/10.1016/S0263-8231(02)00083-6.

[14] H. Liu, J. Hu, Y. Yang, Z. Chen, and L. Wang, "Circular steel tubes strengthened by welding angle steel under preloading condition," *Journal of Constructional Steel Research*, vol. 184, Sep. 2021, Art. no. 106816, https://doi.org/10.1016/j.jcsr.2021.106816.